# Friction drag on a particle moving in a nematic liquid crystal

R. W. Ruhwandl and E. M. Terentjev
*Cavendish Laboratory, University of Cambridge, Madingley Road, Cambridge CB3 0HE, United Kingdom*
(Received 22 April 1996)

The flow of a liquid crystal around a particle not only depends on its shape and the viscosity coefficients but also on the direction of the molecules. We studied the resulting drag force on a sphere moving in a nematic liquid crystal MBBA (4-methoxybenzlidene-4′-*n*-butylaniline) in a low Reynold's number approach for a fixed director field (low Ericksen number regime) using the computational artificial compressibility method. Taking the necessary disclination loop around the sphere into account, the value of the drag force anisotropy ($F_\perp/F_\parallel=1.50$) for an exactly computed field is in good agreement with experiments ($\sim 1.5$) done by conductivity diffusion measurements. We also present data for weak anchoring of the molecules on the particle surface and of trial fields, which show to be sufficiently good for most applications. Furthermore, the behavior of the friction close to the nematic to isotropic transition point and for a rodlike and a disklike liquid crystal will be given. [S1063-651X(96)04411-X]

PACS number(s): 61.30.Jf, 61.30.Cz, 83.85.Pt

## I. INTRODUCTION

Most of the applications of liquid crystals are connected to their flow properties, either while processed or in the application itself. The reorientation of the director field, for example, which is used in electro-optical devices, is linked to internal flow. The fastest response times needed for further development are limited by the friction effects. But although the basics of the hydrodynamics of liquid crystals were established about 30 years ago, most of the problems connected with flow are still unsolved. This is mainly due to the anisotropy of the system and the nontrivial connection of the direction of the molecules and the velocity.

A deeper insight into the hydrodynamics of liquid crystals and the connection between macroscopic and microscopic properties would allow one to predict the behavior of particular materials and therefore to design special liquid crystals to obtain certain characteristics required. Precision experiments are often difficult to perform since many of the standard techniques do not work for these materials. It would be useful to have more independent methods of measuring the viscosity than only a traditional shear flow. A further technique, the falling ball experiment, was solved for an isotropic liquid by Stokes. It consists of a ball falling down in a cylinder driven by the gravitational force and measuring its equilibrium velocity. The viscosity $\eta$ can then be determined by the well-known Stokes formula $F_D=-6\pi r\eta v$, which gives the relation between the friction drag $F_D$, the radius $r$ of the ball, and its velocity $v$.

For liquid crystals this problem gets another dimension since the drag force also depends on the geometry of the system. It is obvious that the drag force on the sphere is different for the two particular cases of the flow and director parallel and the flow and director perpendicular to each other. Using a liquid crystal of rodlike molecules, it becomes clear that it is easier to move the particle parallel to the general director field, i.e., along the long axis of the molecules, than to move it perpendicular to the director, i.e., perpendicular to the long axis. In the general case (arbitrary angle between flow and director) this results in the fact that the drag force is no longer parallel to the line of motion. There is a further component perpendicular to it, the so-called lift force, which moves the particle sideways (see Fig. 1). It is worth mentioning that this force does not contribute to the dissipative losses in the system, an effect well known from other areas of physics such as electrodynamics (a charged particle in a magnetic field is forced to change its direction without losing or gaining any kinetic energy).

A further problem is the influence of the director field $\hat{\mathbf{n}}(\mathbf{r})$ on the flow since it not only changes but also gives a contribution to the dissipative losses in the systems. In particular, regions of high gradients of the director field result in higher resistance to the flow. Such regions are mainly found around disclinations, which are often unavoidable due to the geometry of the system. If we consider, for example, perpendicular boundary conditions on the surface of the sphere and a uniform director field far away from it, there is a disclination loop around the sphere (see Fig. 1), which is unavoid-

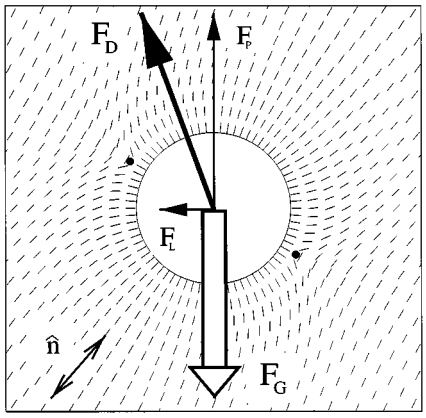


FIG. 1. If a sphere falls down in a gravitational field and the director field is not parallel to the force, there is, besides the friction $F_p$ antiparallel to the gravitational force, also a component $F_L$ perpendicular to it, the so-called lift force. Note also the disclination loop around the particle due to the boundary conditions, indicated by the dots.

 

able for topological reasons. The surface of the sphere corresponds to a $s=1$ point defect and since the overall defect charge of the system must be zero (the director field is uniform far from the particle) this defect must be balanced by the disclination loop. The energy of the ring is roughly proportional to its length, therefore it is favorable to have it as small as possible. On the other hand, the rigid boundary conditions at the surface of the particle push the ring away from the sphere, so that the final position is given by the balance of the two effects.

The drag force is sensitive to the radius of this loop. In both limiting cases (flow and director parallel or perpendicular to each other) the resistance is increased, but the magnitude of the influence is quite different. For the director perpendicular to the velocity the flow is parallel to the ring and it acts like a plate moving in the liquid crystal. For the velocity and (general) director parallel to each other the flow is perpendicular to the ring, which not only increases the cross section of high director gradients around the ring and the liquid crystal flow but also has a further effect: a certain amount of the liquid crystal has to flow through the gap between the ring and sphere, where the director lies in the plane of the ring and is therefore locally perpendicular to the direction of the flow. As a consequence, the anisotropy of the system, i.e., the ratio of the drag forces, decreases with an increasing radius of the disclination loop. This means that stronger boundary conditions lower the anisotropy.

The theoretical problem of a liquid crystal flowing around a body has been addressed before. Diogo [1] assumed the velocity field around the sphere to be the same as for an isotropic fluid and calculated the drag force for different angles between the director and the velocity. Roman and Terentjev [2] obtained an analytic solution for the flow velocity for a fixed uniform director field, by an expansion in the anisotropy of the viscosity. Recently, Heuer, Kneppe, and Schneider gave solutions for the velocity of the liquid crystal, assuming a uniform director field, independent of the flow [3].

All these solutions have their deficiencies. None of them, for instance, considered the distribution of the director field due to the boundary conditions on the particle. This will be done in this article, where the results are also compared with various approximations for the director $\hat{\mathbf{n}}(\mathbf{r})$.

The article is organized as follows. After a brief introduction to the basic equations of the hydrodynamics of liquid crystals that are needed in Sec. II, we give, in Sec. III, a short description of the numerical method we used to solve the equations of motion. Section IV gives the director fields we used and explains the limits when they are valid. The results for the drag properties and a comparison with experimental data are given in Sec. V and, finally, we conclude with a discussion of possible experiments in Sec. VI.

## II. BASIC CONCEPTS

In this section we give a brief summary of the nematic hydrodynamics that are used in this work. For derivations of these equations we refer the reader to the basic textbook [4]; see also [5]. The stress tensor of a nematic liquid crystal consists of three contributions. The first two are the hydrodynamic pressure $p$ and the viscous stress given by the tensor

$$\sigma'_{ij}=\alpha_1 n_i n_j n_k n_l A_{kl}+\alpha_2 n_j N_i+\alpha_3 n_i N_j+\alpha_4 A_{ij}+\alpha_5 n_j n_k A_{ik}+\alpha_6 n_i n_k A_{jk}. \quad (1)$$

(Here and below in this article we use the tensor index notation, i.e., an index appearing twice in a product means a summation over this index, and the shorthand notation for gradients $B_{,j}\equiv\nabla_j B$). Here $\alpha_i$ are the viscosity (Leslie) coefficients, $\mathbf{A}$ represents the symmetric part of the fluid velocity gradients $[A_{ij}=\frac{1}{2}(v_{i,j}+v_{j,i})]$, and the vector $N_i=\dot{n}_i+\frac{1}{2}[\hat{\mathbf{n}}\times\mathrm{curl}\mathbf{v}]_i$ is the change of the director with respect to the background fluid. Finally, there is a static (elastic) contribution due to the curvature of the director field

$$\sigma^e_{ij}=-Kn_{k,j}n_{k,i}, \quad (2)$$

given in the one-constant approximation (Frank elastic constants $K_1=K_2=K_3\equiv K$).

The director field is determined by the balance between the static molecular field $\mathbf{h}^0=K\nabla^2\hat{\mathbf{n}}$ and the viscous molecular field $h'_i=(\alpha_2-\alpha_3)N_i+(\alpha_6-\alpha_5)n_jA_{ij}$. The total molecular field has to be parallel to the director, but $h'$ can be neglected in the low Ericksen number regime [5] ($\mathrm{Er}=\alpha vR/K\ll 1$, where $v$ is a characteristic velocity and $R$ the radius of the sphere). This condition is met in a typical thermotropic liquid crystal with $K\sim 10^{-11}$ N; $\alpha\sim(5-10)\times 10^{-2}$ Pa s in the case of $vR\ll 10^{-8}$ m$^2$ s$^{-1}$, which allows speeds of mm/s for small colloid particles ($R\sim 10$ $\mu$m).

Considering low Reynolds number flow and using the equation of continuity we end up with seven equations

$$\sigma_{ij,j}=0, \quad (3)$$

$$v_{i,i}=0, \quad (4)$$

$$Kn_{i,jj}=\lambda n_i \quad (5)$$

for seven unknown variables (three for the velocity field $\mathbf{v}$, three for the director $\hat{\mathbf{n}}$ and the Lagrange multiplier $\lambda$ constraining $\hat{\mathbf{n}}^2=1$, and one for the pressure). The equation (5) for the director is decoupled from the velocity due to the low Ericksen number approach and can be solved separately for the static problem, which then leaves only the hydrodynamic part of Eqs. (3) and (4). Once the velocity field $\mathbf{v}(\mathbf{r})$ and the pressure $p(\mathbf{r})$ are obtained, the convenient way to determine the drag force is by calculating the total dissipation in the system

$$Fv_\infty=\int(\boldsymbol{\sigma}':\mathbf{A}+\mathbf{h}'\cdot\mathbf{N})dV, \quad (6)$$

where $v_\infty$ is the constant velocity of the fluid at infinity.

## III. NUMERICAL METHOD

We followed the example of Heuer, Kneppe, and Schneider [3] and used the artificial compressibility method (see, for example, [6]) to solve the equations of motion. The idea of this method is that the system starts with an arbitrary startup velocity and pressure field and relaxes in an artificial time towards its equilibrium, which is the solution we are

TABLE I. Treatment of the boundaries around the first octant. The notation bc refers to the fact that this value is fixed by the boundary conditions of the problem, symm denotes given by symmetry, the values given by cal can be calculated with the untreated equations of motion, se-inter is the value determined by an analytically simplified equation for the uniform field and by an interpolation for the nonuniform field, and finally extr means the value was calculated by an extrapolation.

| | $\xi=0$ | $\xi=1$ | $\phi=0$ | $\phi=\frac{\pi}{2}$ | $\theta=0$ | $\theta=\frac{\pi}{2}$ |
|---|---|---|---|---|---|---|
| $\mathbf{v}_x$ | bc→0 | bc→0 | cal | symm→0 | symm→0 | symm→0 |
| $\mathbf{v}_y$ | bc→0 | bc→0 | symm→0 | cal | bc→0 | bc→0 |
| $\mathbf{v}_z$ | bc→1 | bc→0 | cal | cal | se-inter | cal |
| $\mathbf{p}$ | bc→0 | extr | cal | cal | se-inter | bc→0 |

looking for ($\partial_t p=0$, $\partial_t v_i=0$). The equations to solve are

$$\sigma_{ij,j}=\partial_t v_i, \quad v_{i,i}=-c^2\partial_t p, \tag{7}$$

where $c$ is an arbitrary damping parameter, which should be chosen as large as possible to speed up the calculation (however, if $c$ is too large the numerical scheme becomes unstable).

Due to the linearity of Eqs. (7) it is necessary to solve them only for the two particular cases where the flow and director are parallel and perpendicular to each other [$\hat{\mathbf{n}}(\infty)\|\mathbf{v}(\infty)$ and $\hat{\mathbf{n}}(\infty)\perp\mathbf{v}(\infty)$]. The advantage of these solutions is the simple geometry. For an arbitrary angle between the velocity and director they are just added together, i.e., the friction drag can be calculated by the resistance tensor $M_{ij}=M_\perp\delta_{ij}+(M_\parallel-M_\perp)n_i n_j$, which determines the response of the drag force on the sphere to the flow around it:

$$F_i=M_{ij}(\hat{\mathbf{n}})v_{\infty j}=M_\perp v_{\infty i}+(M_\parallel-M_\perp)(\mathbf{v}_\infty\cdot\hat{\mathbf{n}})n_i.$$

For an isotropic liquid the tensor is simply $M_{ij}=M\delta_{ij}$, where the constant $M$ is given by the Stokes friction $M=-6\pi R\eta$. The ratio $M_\perp/M_\parallel$ is a measure for the anisotropy in the system since this gives the lift effect in the drag force. In the first case, assuming that the flow is along the $z$ axis and the director is parallel to it, the system is symmetric with respect to azimuthal rotations around the $z$ axis. When the velocity components are transformed to cylindrical components ($v_x,v_y,v_z\rightarrow v_\rho,v_\phi,v_z$) the azimuthal velocity $v_\phi$ is zero everywhere in the system and the problem becomes two dimensional. Furthermore, it is favorable to use a spherical coordinate system with an inverse radius ($\xi=1/r=1/\sqrt{x^2+y^2+z^2}$, $\theta=\arctan\sqrt{x^2+y^2}/z$, and $\phi=\arctan y/x$). This has two advantages: the outer boundary conditions [$\mathbf{v}(\infty)$, $p(\infty)$] are included in the grid used for the calculations and the mesh size of the grid is smaller near the surface of the sphere, where most of the changes happen, and large far from the particle, where the values stay almost constant. It is sufficient to pursue the calculations in one quadrant only since the other three are given by symmetry. It is also evident that the radial velocity must be zero at both boundaries. The values for $v_z$ at $\theta=\pi/2$ can be computed as the inner grid points, whereas the values at $\theta=0$ request special treatment since they contain the term $\cos\theta$ and are therefore of the form 0/0. Since it was not possible to obtain them by an interpolation, we simplified the equation by taking the limit for $\theta=0$ [$v_z(\xi,0)=\lim_{\theta\rightarrow 0}v_z(\xi,\theta)$] analytically (application of l'Hôpital's rule).

In the second case, the director perpendicular to the velocity, there is no rotational symmetry and the calculations have to be done on a three-dimensional grid. It is again favorable to use spherical coordinates with an inverse radius (see Fig. 1) for the reasons explained above, but this time the velocity components are kept Cartesian [i.e., $v_x(\xi,\phi,\theta),v_y(\xi,\phi,\theta),v_z(\xi,\phi,\theta)$]. Due to the symmetry it is sufficient to solve the equations in one octant. The conditions on the boundaries of this octant and the needed values are calculated as is shown in Table I.

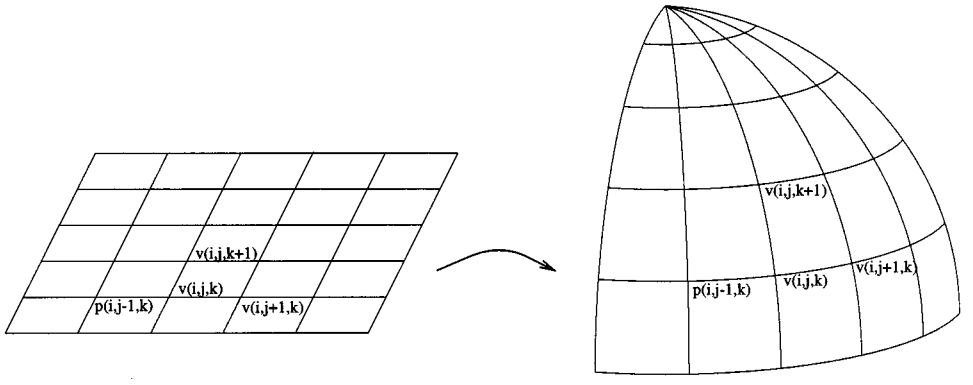


FIG. 2. One layer of the matrix ($\xi=1/\mathbf{r}=$const) and its transformation to real space. The lines of the constant angle $\phi$ transform to longitudes and the constant $\theta$ to latitudes. Note the decreasing distance between two longitudes while approaching the pole. This yields a nonunique point at $\theta=0$.

The constant number of grid points in the plane of the azimuthal angle $\phi$ direction (independent of $\theta$) leads to a decrease in the mesh size in real space while approaching the pole and finally yields a nonuniqueness for the pole ($\theta=0$) itself. A constant distance in real space would require fewer points (a factor $\sim 0.7$), but it involves more calculations since the derivatives become more difficult. Therefore we chose the grid shown in Fig. 2. The values at the $z$ axis, which are nonunique, were then calculated for each $\phi$ and set to their average over $\phi$ [$v_z(\xi,\phi,0)=\langle v_z(\xi,\phi,0)\rangle_\phi$ for every $\xi$].

## IV. DIRECTOR FIELD

As described above, the director field can be taken as fixed during the calculations in the low Ericksen number regime. In order to study the influence of simplifying assumptions concerning the form of the field we performed the calculations with different director fields $\hat{\mathbf{n}}(\mathbf{r})$. In the one-constant approximation the director field is described by the minimum of the Frank free energy $F_d$

$$F_d=\int (\nabla\cdot\hat{\mathbf{n}})^2+(\nabla\times\hat{\mathbf{n}})^2 dV. \tag{8}$$

If we take into account that $\hat{\mathbf{n}}$ is a unit vector and set $\hat{\mathbf{n}}(\infty)$ parallel to the $z$ axis, we can write the director components as

$$n_x=\sin\beta\,\sin\gamma, \tag{9}$$

$$n_y=\sin\beta\,\cos\gamma, \tag{10}$$

$$n_z=\cos\beta, \tag{11}$$

where $\beta$ and $\gamma$ are angles dependent on the spatial coordinates. The director field in our problem is rotationally symmetric with respect to the $z$ axis. We can therefore set $\gamma=\arctan y/x$. Inserting this into Eq. (8) and minimizing it, we are left with one equation for the polar angle $\beta(\mathbf{r})$:

$$\nabla^2\beta-\frac{\sin 2\beta}{2r^2\sin^2\theta}=0, \tag{12}$$

where $\beta$ is a function of the radius $r$ and the azimuthal angle $\theta$. There are several possibilities to proceed with finding the static director field (see Fig. 3).

(i) If we neglect the boundary conditions on the surface (anchoring energy is zero) we get the (trivial) solution $\beta(r,\theta)\equiv 0$, i.e., the director is uniform in space, parallel to the $z$ axis. This was the approach chosen by Heuer, Kneppe, and Schneider authors [3] in their analysis.

(ii) Provided the anchoring on the surface is weak and therefore the angle $\beta$ [the deviation from $\hat{\mathbf{n}}(\infty)$] remains small, Eq. (12) can be linearized and yields

$$\nabla^2\beta-\frac{\beta}{r^2\sin^2\theta}=0. \tag{13}$$

This equation, with the corresponding boundary conditions and the symmetry of the problem, can be easily solved and gives $\beta=(RW/4K)R^3\sin 2\theta/r^3$, where $W$ is the anchoring energy and $R$ the radius of the particle [7].

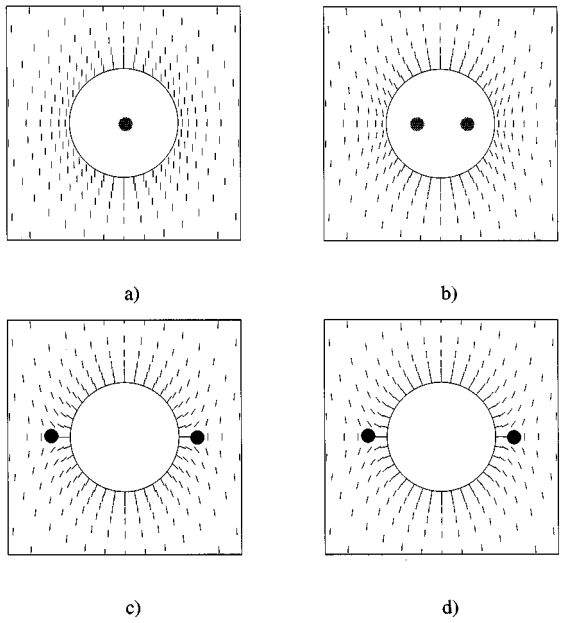


FIG. 3. Director fields for (a) no anchoring at the surface of the sphere, (b) weak anchoring, (c) arctan field, and (d) numerical solution fulfilling the boundary conditions. The black dots show the position of the disclination loop and the gray dots show where they would be (having this director field without the sphere).

(iii) If we assume strong anchoring on the surface of the sphere ($WR/K\gg 1$) the director field is forced to have a disclination loop (radius $a$) around the equator of the field. The direction of the molecules in the plane of the ring must be radial between the ring and disclination and parallel to the $z$ axis in this plane outside the disclination. Furthermore, the perturbation of the field must decay as $1/r^3$ far from the sphere. The simplest function that shows this behavior is

$$\beta=\theta-\frac{1}{2}\arctan\frac{\sin 2\theta}{\cos 2\theta+\left(\frac{a}{r}\right)^3}. \tag{14}$$

There is an extensive discussion of the features and details of the director field in the strong anchoring regime [7]. The conclusion reached [7] is that Eq. (14) provides a very good approximation, describing well the far-field behavior, the disclination ring vicinity, and even the weak anchoring case when the ring radius $a$ is taken $a\rightarrow WR^4/4K$.

(iv) There is no analytical solution for the whole problem [satisfying Eq. (12) *and* the boundary conditions]. We therefore solved the equilibrium equation (12) numerically with a method similar to the artificial compressibility method mentioned before. In this way we obtain the exact director field $\hat{\mathbf{n}}(\mathbf{r})$ on every point of our grid.

## V. RESULTS

First we examine the influence of the different director fields [uniform, trial function $\beta$, and the exact numerical $\hat{\mathbf{n}}(\mathbf{r})$] on the drag force acting on the sphere, using the par-

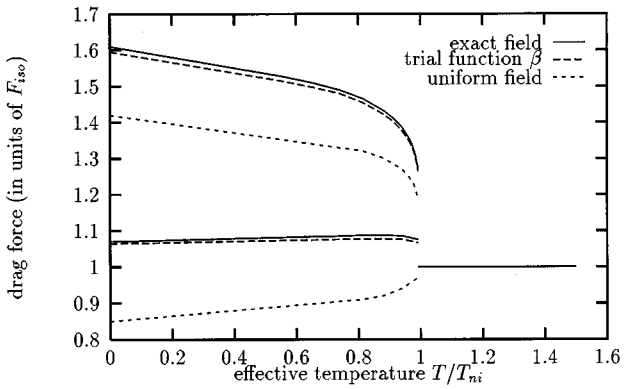


FIG. 4. Drag force on the sphere for three different director fields (uniform, trial, and real field) depending on the effective temperature $T/T_{ni}$. The upper lines are for the case of the director and velocity parallel and the lower ones for the director and velocity perpendicular to each other.

ticular set of viscous coefficients of 4-methoxybenzlidene-4′-*n*-butylaniline (MBBA) [4]. As expected, the uniform field shows a much lower drag force for both principal configurations of $\hat{\mathbf{n}}(\infty)$ and $v(\infty)$ than the trial field and the exact field; see Fig. 4 (for the velocity parallel to the director it is even smaller than for the isotropic drag force). On the other hand, the anisotropy of the drag forces (the ratio of the two forces $F_\perp/F_\parallel$) becomes smaller for the realistic nonuniform field. This is due the following: the flow velocity around the sphere is highest in the region of the equator plane perpendicular to the line of motion. If the liquid crystal is oriented along the same $z$ axis we get a very high gradient of the director in exactly the same region due to the effect of the disclination ring. In the other principal configuration, where the director $\hat{\mathbf{n}}(\infty)$ is perpendicular to the $z$ axis and therefore perpendicular to the velocity, the disclination with its high gradients is the same, but this time the loop is around a longitude of the sphere. It still increases the drag, but in a much smaller region since the flow velocity at the stagnant poles is almost zero already. The anisotropy in the drag force for the three director fields yields

$$\left.\frac{F_\perp}{F_\parallel}\right|_{\text{uniform}}=1.69,\quad \left.\frac{F_\perp}{F_\parallel}\right|_{\text{trial}\beta}=1.50,\quad \left.\frac{F_\perp}{F_\parallel}\right|_{\text{exact}}=1.50. \tag{15}$$

The results obtained with the trial field are surprisingly close to those of the exact director field. They obviously reflect the important features of the field that are mainly the disclination loop and the $1/r^3$ decay of the deviation in the angle far from the particle, whereas the particular details near the particle and the disclination seem to be of minor importance. Therefore, the drag force is determined by the long-range effects. The difference between the drag force of the trial functions and the drag force obtained from the exact numerical solution is less than 1% and the difference in the force ratios is smaller than the accuracy of the calculations. In most practical cases it should be sufficiently accurate to use these trial $\hat{\mathbf{n}}(\mathbf{r})$ fields instead of a numerical solution of the governing equations. The uniform field, on the other hand, is not a very useful assumption since its resulting drag force differs from that for the exact $\hat{\mathbf{n}}(\mathbf{r})$ distribution by up to 20%. The significantly higher ratio is a particular problem since it shows that the effect of boundary conditions on the surface cannot be simply modeled by a larger effective hydrodynamic radius. The dependence on the mutual orientation of $n_\infty$ and $v_\infty$ is too strong.

These results can be compared with experimental figures. The diffusion of particles in a nematic liquid crystals [8] is described by the diffusion tensor $\mathbf{D}$, which is indirectly proportional to the resistance tensor, $\mathbf{D}=k_BT(\mathbf{M})^{-1}$, where $k_B$ is the Boltzmann factor and $T$ the temperature. Consequently, the tensor is of the same form as the mobility tensor $D_{ij}=D_\perp\delta_{ij}+(D_\parallel-D_\perp)n_in_j$, with $D_\perp=k_BT/M_\perp$ and $D_\parallel=k_BT/M_\parallel$. Recent experiments [9] showed for the self-diffusion constants of MBBA a ratio of $D_\parallel/D_\perp\sim1.5$. Easier to determine experimentally is the anisotropy in the electric conductivity [12] $\boldsymbol{\mu}$ of a sample, which is related to the diffusion by

$$\mathbf{D}=\frac{k_BT}{ne^2}\boldsymbol{\mu} \tag{16}$$

for $n$ charge carriers of charge $e$ per $\text{cm}^3$. The conductance anisotropy was often measured [4] and for MBBA it is usually equal to $\mu_\parallel/\mu_\perp\sim1.5$. Both experiments are in excellent agreement with our result for $M_\perp/M_\parallel=1.50$.

The dependence of the drag force on the temperature is also of great interest in many experiments. The viscous coefficients $\alpha_1$, $\alpha_2$, $\alpha_3$, $\alpha_5$, and $\alpha_6$, in the first approximation, depend linearly on the order parameter $S$ in the region close to the nematic to isotropic transition temperature $T_{ni}$. The order parameter $S$ itself can be approximated by Haller's equation [10]

$$S=\Delta S+\left(1-\frac{T}{T_{ni}}\right)^\gamma, \tag{17}$$

where $\gamma$ is determined experimentally for MBBA [11] to be $\gamma=0.188$. The viscous coefficients scale, therefore,

$$\alpha_1\to\alpha_1S,\quad \alpha_2\to\alpha_2S,\quad \alpha_3\to\alpha_3S,$$
$$\alpha_4\to\alpha_4,\quad \alpha_5\to\alpha_5S,\quad \alpha_6\to\alpha_6S. \tag{18}$$

The drag force shows, for the perpendicular case, more or less the same behavior for all director fields: after a jump at the transition point, it increases while lowering the temperature, in the beginning rapidly, then slower and slower. On the other hand, there is a qualitative change for the parallel drag force: while it jumps to a lower value and then decreases further for the uniform field, it shows a small change to a higher value at the transition point at which it stays almost constant independent of the temperature, for both the trial field of $\beta$ and the exact field (see Fig. 4).

The boundary conditions are not absolutely rigid in many experiments due to a finite anchoring energy, in which case the approximative director field (13) can be used. A typical colloidal particle of radius $R=10^{-5}$ m in a liquid crystal with an elastic constant of $K\sim10^{-11}$ N has an anchoring energy of $W\sim10^{-5}$–$10^{-7}$ $\text{J/m}^2$. This corresponds to a relevant dimensionless factor of $WR/K=0.1$–$10$. Our calcula-

tions showed a slow linear increase of the drag forces $F_\perp$ and $F_\parallel$ in the range of weak anchoring, $WR/K=0-4$ due to the deviation of the director field from the uniform state. This results in gradients in the field that increase the dissipation and therefore the resistance of the particle to the flow. The effect on the force in the parallel case $F_\parallel$ is obviously stronger than in the perpendicular case $F_\perp$, which is reflected in a linear decrease of the anisotropy ratio $F_\perp/F_\parallel$ while enlarging the anchoring energy $W$.

The authors of [7] have also examined the case of charged particles, when the radial electric field near the surface forces the disclination loop to be pushed further away from the particle. An approximate expression for the loop radius $a$ is then given by

$$a^2=\frac{\epsilon_a q^2}{32\epsilon^2(5K+K_{13}-2K_{24})}, \tag{19}$$

where $\epsilon_a$ is the dielectric constant, $q$ the charge of the sphere, and $K_{13}$ and $K_{24}$ elastic constants (assuming no immediate screening). One expects an increase in the drag forces and a decrease in their ratio since the hydrodynamical effective cross section of large director gradients is increased far more for the parallel case than for the perpendicular one. For instance, taking the loop radius $a\sim 2R$, the results for the MBBA set of Leslie coefficients are

$$F_\perp=1.75F_{\rm iso}, \quad F_\parallel=1.23F_{\rm iso}, \quad \frac{F_\perp}{F_\parallel}=1.43, \tag{20}$$

where the drag forces are given in units of MBBA in the isotropic phase $F_{\rm iso}=-6\pi R\eta v$ using $\eta=0.5\alpha_4$ as the viscosity coefficient. As mentioned above, the anisotropy of the drag forces decreases with increasing the strength of the boundary conditions from $F_\perp/F_\parallel=1.69$ for the uniform field (anchoring energy $W=0$), followed by a slow linear increase for weak anchoring ($WR/K\ll 1$), and $F_\perp/F_\parallel=1.5$ for rigid anchoring to $F_\perp/F_\parallel=1.43$ for the case of the charged particle, which can be considered as ''overly strong'' anchoring.

The molecular characteristics of the liquid crystal are inherent in the viscous coefficients. These coefficients depend, among other things, on the shape of the molecules that form the liquid crystal. This influence can be modeled by an affine transformation model [13] giving the viscous coefficients depending on the molecular aspect ratio $l_\parallel/l_\perp$:

$$\alpha_1=-\frac{1}{2}\alpha_0\left(\frac{l_\parallel}{l_\perp}-\frac{l_\perp}{l_\parallel}\right)^2, \quad \alpha_2=\frac{1}{2}\alpha_0\left(1-\left[\frac{l_\parallel}{l_\perp}\right]^2\right),$$

$$\alpha_3=\frac{1}{2}\alpha_0\left(\left[\frac{l_\perp}{l_\parallel}\right]^2-1\right), \quad \alpha_4=\alpha_4, \quad \alpha_5=-\alpha_2, \quad \alpha_6=\alpha_3. \tag{21}$$

Baalss and Hess [13] determined the aspect ratio of MBBA to be $l_\parallel/l_\perp=5/2$. We used this value to obtain the constant $\alpha_0$ by comparing the largest coefficient $\alpha_2$ with the experimental value and the isotropic coefficient $\alpha_4$ was taken from MBBA directly. We calculated the example cases of two particular configurations: a rodlike molecule with ratio $l_\parallel/l_\perp=7/2$ and a disklike system $l_\parallel/l_\perp=3/5$. The results of these calculations are

$$F_\perp=2.33F_{\rm iso}, \quad F_\parallel=1.78F_{\rm iso},$$

$$\frac{F_\perp}{F_\parallel}=1.31 \ \text{(rodlike molecule)},$$

$$F_\perp=0.94F_{\rm iso}, \quad F_\parallel=1.52F_{\rm iso},$$

$$\frac{F_\perp}{F_\parallel}=0.62 \ \text{disklike molecule}. \tag{22}$$

Note the inverted ratio of the drag forces for the disklike molecules.

## VI. CONCLUSION

Considering the low Ericksen number regime ($\mathrm{Er}=\alpha v R/K\ll 1$) the director field can be taken as independent of the flow in the first approximation. We therefore took several static director fields (approximations for the field in the limit of strong and weak anchoring and the solution of the governing equations). The equations of motion were then solved numerically for the different fields $\hat{\mathbf{n}}(\mathbf{r})$ using the viscous coefficients of MBBA. Due to the linearity of the Eqs. (7) it is only necessary to solve two limiting case, for the director and velocity parallel and perpendicular to each other at infinity [$\hat{\mathbf{n}}(\infty)\|\mathbf{v}(\infty)$ and $\hat{\mathbf{n}}(\infty)\perp\mathbf{v}(\infty)$]. This yields the drag forces $F_\parallel$ and $F_\perp$, which can be combined for the general case by the mobility tensor.

The comparison of the drag forces for the different director fields showed that the disclination loop around the sphere, which is topologically necessary for a large anchoring energy of the molecules on the surface, not only increases the forces itself but also decreases their ratio to $F_\perp/F_\parallel=1.50$ compared to a uniform case ($F_\perp/F_\parallel=1.69$). Trial director fields, constructed from the basic features of the director field (the disclination ring and $1/r^3$ decay of the far field), showed to be a very good approximation. The difference between the values of $F_\parallel$ and $F_\perp$ compared to the ones obtained for the exact field is less than 1%.

The temperature dependence of the drag force showed an increase in the force $F_\perp$ for decreasing temperature and an almost constant value for the parallel force ($F_\parallel$). An approximation for the director field for weak anchoring energy shows a linear decrease for lowering the anchoring energy in both particular drag forces as well as in their ratio.

The value for MBBA ($F_\perp/F_\parallel=1.50$), using the exact solution of the director field, is in good agreement with experimental results, measured by the static conductivity and the self-diffusion of MBBA (both $\sim 1.5$).

The disclination loop can be pushed away from the sphere, for instance, in the case of nonscreened charges on the particle. This increases the particular forces compared with the uncharged case, where the loop is close to the surface, and yields, for a loop radius of twice the particle radius, an even lower ratio of $F_\perp/F_\parallel=1.43$.

The viscous coefficients of other materials can be approximated by an affine transformation model, which uses the aspect ratio ($l_\parallel/l_\perp$) of the molecules as parameter. For a rodlike molecule ($l_\parallel/l_\perp=7/2$) we obtained an anisotropy in the drag force of $F_\perp/F_\parallel=1.31$ and for a disklike molecule ($l_\parallel/l_\perp=3/5$) the ratio obtained was $F_\perp/F_\parallel=0.62$. The ratio

smaller than one indicates that the lift force turns the particle away from the director, whereas a ratio larger than one forces the particle in the direction of the director.

It is especially interesting to examine the lift component of the drag force, i.e., the nondissipative force acting perpendicular to the line of particle motion. It resembles magnetic forces and leads to physical phenomena, similar to the Hall effect. In a long cell, the ratio between the cross voltage $U^*$ and the applied voltage $U$ is determined by the anisotropy ratio $V=\mu_\parallel/\mu_\perp$ [12]

$$\frac{U^*}{U}=-\frac{b}{a}\frac{\sin 2\theta}{(V+1)/(V-1)-\cos 2\theta}, \tag{23}$$

where $a$ is the width of the sample (in direction of the applied voltage) and $b$ the thickness of the sample (in direction of the cross voltage). The conductivity is determined by the movement of the charge carriers and therefore inversely proportional to the resistance, which yields, for the anisotropy ratios, $V=M_\perp/M_\parallel=F_\perp/F_\parallel$.

Since it is difficult to produce samples of liquid crystals without disclinations, which are sufficiently large to perform measurements of moving particles, the effect of the lift force (the component of the drag force that is perpendicular to the driving force) could be observed in a long cylinder. If the boundaries force the liquid crystal to be perpendicular to the walls of the cylinder, the director field will ''escape to the third dimension,'' i.e., it will turn around to be parallel to the long axis of the cylinder while approaching its center since this is energetically much more favorable than a disclination line. If the distances with the same well-defined curvature along the $z$ axis are large enough, little spheres, which are dropped in the sample, should show a certain measurable displacement during their way down in a gravitational field.

Further possibilities are the usage of electric and magnetic fields. Moving particles can be guided by changing the director orientation in the sample to direct them to a certain destination in the sample. This enables the guiding of uncharged and unpolarizable particles with electric or magnetic fields.

## ACKNOWLEDGMENTS

The authors have benefited from discussions with C. Bergemann, F. M. Leslie, J. R. Melrose, and M. Warner. This research has been supported by the EPSRC and Unilever PLC.

[1] A. C. Diogo, Mol. Cryst. Liq. Cryst. **100**, 153 (1983).
[2] V. G. Roman and E. M. Terentjev, Colloid J. USSR **51**, 435 (1989).
[3] H. Heuer, H. Kneppe, and F. Schneider, Mol. Cryst. Liq. Cryst. **214**, 43 (1992).
[4] P. G. de Gennes and J. Prost, *Physics of Liquid Crystals*, 2nd ed. (Clarendon, Oxford, 1993).
[5] R. W. Ruhwandl and E. M. Terentjev, Z. Naturforsch. Teil A **50**, 1023 (1995).
[6] R. Peyret and T. D. Taylor, *Computational Methods for Fluid Flow* (Springer, New York, 1983).
[7] O. V. Kuksenok, R. W. Ruhwandl, S. V. Shiyanovskii, and E. M. Terentjev, preceding paper, Phys. Rev. E **54**, 5198 (1996).
[8] A. Böttger, D. Frenkel, E. van de Riet, and R. Zijlstra, Liq. Cryst. **2**, 539 (1987).
[9] K. Ohta, T. Masahide, and H. Noboru, Bull. Chem. Soc. Jpn. **68**, 2809 (1995).
[10] I. Haller, Prog. Solid State Chem. **10**, 103 (1975).
[11] H. Kneppe, V. Reifenrath, and F. Schneider, Chem. Phys. Lett. **87**, 59 (1982).
[12] G. Heppke and F. Schneider, Chem. Phys. Lett. **13**, 548 (1972); **27a**, 976 (1972).
[13] D. Baalss and S. Hess, Z. Naturforsch. Teil A **43**, 662 (1988).